



(CuBr)₂P₈Se₃: preparation, structural, and vibrational spectroscopic characterization of an adduct of P₈Se₃ cages to Cu₂Br₂ rhombs

S. Nilges^a, T. Nilges^a, H. Haeuseler^b, A. Pfitzner^{a,*}

^aInstitut für Anorganische Chemie, Universität Regensburg, Universitätsstraße 31, 93040 Regensburg, Germany

^bInstitut für Anorganische Chemie, Universität Siegen, 57068 Siegen, Germany

Received 30 December 2003; revised 29 January 2004; accepted 29 January 2004

Dedicated to Prof. Dr H.D. Lutz on the occasion of his 70th birthday

Available online 28 March 2004

Abstract

Orange–red (CuBr)₂P₈Se₃ was obtained from stoichiometric amounts of CuBr, P and Se by melting and subsequent annealing at 380 °C for 1 month. The crystal structure was determined from single crystal X-ray data. (CuBr)₂P₈Se₃ crystallizes in the orthorhombic system, space group *Pbcm* (No. 57), with $a = 8.761(1)$ Å, $b = 11.957(1)$ Å, $c = 13.858(1)$ Å, $V = 1451.8(3)$ Å³, and $Z = 4$. This compound consists of neutral P₈Se₃ cage molecules attached to Cu₂Br₂ rhombs. Vibrational spectroscopic data are reported for (CuBr)₂P₈Se₃ and for the homologous (CuI)₂P₈Se₃. The wavenumbers of the Cu–Br and Cu–I vibrational modes show an excellent correlation with the corresponding Cu–X bond lengths.

© 2004 Elsevier B.V. All rights reserved.

Keywords: Phosphorus chalcogenide; Copper; Halide; Vibrational spectroscopy; X-ray diffraction; Crystal structure

1. Introduction

Copper(I) halides have been established as a useful tool for the synthesis of hitherto unknown main group molecules and low charged polyanions [1]. These adduct compounds are of special interest because they show an enhanced ionic mobility due to only weak bonding interactions between copper and the neutral ligands [2]. Thus, a number of phosphorus polymers, chalcogen molecules and phosphorus chalcogenides could be obtained as their adducts to copper(I) halides. Recently, even an arsenic substituted phosphorus polymer embedded in CuI was reported [3]. In addition to their ion conducting properties, these compounds can be used as model compounds for the basic characterization of copper containing phosphorus chalcogenide glasses by solid state NMR spectroscopy [4]. Whereas the chalcogen polymers

and chalcogen rings were obtained as adducts to CuCl, CuBr, and CuI the phosphorus containing compounds are usually based on CuI but never on CuCl and only in a few cases on CuBr, see Ref. [1]. Different compounds were observed, e.g. for CuX with phosphorus polyanions in dependence on X, namely Cu₃P₁₅I₂ [5] and Cu₁₂P₂₀Br₁₀ [6]. In case of the adducts of β-P₄Se₄ with CuX the resulting compounds have an analogous composition, i.e. (CuX)₃P₄Se₄ (X = Br, I) [7,8] but the crystal structures of these compounds differ significantly. When β-P₄S₄ is regarded instead of the β-P₄Se₄ cage (CuI)₃P₄S₄ results which is more or less isostructural with (CuI)₃P₄Se₄ [9]. Obviously different parameters as, e.g. the volume ratios of the constituent building groups, cf. [10], and the coordination modes of the phosphorus chalcogenide cages have to be taken into account when the crystal structures of these adduct compounds are discussed. Herein, we report on the synthesis and the structural and vibrational spectroscopic characterization of (CuBr)₂P₈Se₃ and discuss this compound in comparison with the iodine homologue (CuI)₂P₈Se₃ [11].

* Corresponding author. Tel.: +49-941-943-4552; fax: +49-941-943-4983.

E-mail address: arno.pfitzner@chemie.uni-regensburg.de (A. Pfitzner).

2. Experimental

2.1. Preparation

(CuBr)₂P₈Se₃ was prepared from a 2:8:3 mixture of CuBr (Riedl de Haen, >99%), P (Hoechst, ultra high grade 99.9999%) and Se (Chempur, 99.999%). CuBr was purified by recrystallization from concentrated aqueous HBr (Fluka, purum p.a.) prior to use. The mixture was heated in an evacuated silica tube up to 873 K and kept at this temperature for several hours. Since the mixture was completely molten the temperature was reduced to 653 K. The compound was annealed at this temperature for 30 days. From DSC (SETARAM TG-DTA 92-16) measurements a peritectical decomposition temperature of 680 K was determined for (CuBr)₂P₈Se₃.

2.2. X-ray crystallography

The purity of (CuBr)₂P₈Se₃ was checked by X-ray powder diffraction using a STOE STADIP diffractometer (Cu Kα₁ radiation, Germanium monochromator) equipped with a linear 5° PSD. An orthorhombic unit cell with lattice constants of $a = 8.761(1) \text{ \AA}$, $b = 11.957(1) \text{ \AA}$, $c = 13.858(1) \text{ \AA}$, and $V = 1451.8(3) \text{ \AA}^3$ was calculated from powder diffraction data.

The crystal structure of (CuBr)₂P₈Se₃ was determined by single crystal X-ray diffraction. Intensities of suitable crystals were recorded on a STOE IPDS (Mo Kα radiation, $\lambda = 0.71073 \text{ \AA}$, graphite monochromator) at 298(1) K. A numerical absorption correction was applied after the optimization of the crystal shape based on symmetry equivalent reflections using the XRED and XSHAPE routines [12]. Intensities were averaged in the Laue group *mmm* and the space group *Pbcm* was derived from systematic extinctions. Due to the similarities in lattice parameters and the symmetry with the homologue (CuI)₂P₈Se₃ ($a = 9.1348(6) \text{ \AA}$, $b = 12.351(1) \text{ \AA}$ and $c = 13.873(1) \text{ \AA}$, $V = 1565.2(2) \text{ \AA}^3$, space group *Pbcm* [11]) an isotypic structure was assumed for (CuBr)₂P₈Se₃. Therefore, the atomic positions of (CuI)₂P₈Se₃ were used as a starting model for the structure refinement. The crystal structure was refined with the JANA2000 [13] program package. It converged at $R = 0.0404$ and $wR = 0.0902$ (for reflections with $I > 3\sigma_I$) after anisotropic treatment of all atoms. Crystallographic data, atomic coordinates and anisotropic displacement parameters are summarized in Tables 1–3.

2.3. Vibrational spectroscopy

Far infrared spectra were recorded on a Bruker 113v FT-IR spectrometer. Finely powdered samples were measured as nujol mulls on polyethylene plates with a resolution of 2 cm^{-1} .

Table 1

Crystallographic data of (CuBr)₂P₈Se₃

Compound	(CuBr) ₂ P ₈ Se ₃
Formula weight (g/mol)	771.6
Crystal size (mm ³)	0.08 × 0.07 × 0.06
Temperature (K)	298
Crystal system	Orthorhombic
Space group	<i>Pbcm</i> (No. 57)
Lattice constants (Å) from powder data	$a = 8.761(1)$ $b = 11.957(1)$ $c = 13.858(1)$
Cell volume (Å ³), Z	1451.8(3), 4
ρ_{calc} (g/cm ³)	3.5290(6)
$\mu_{\text{X-ray}}$ (mm ⁻¹)	16.799
Diffractometer	STOE IPDS, Mo Kα, $\lambda = 0.71073 \text{ \AA}$, oriented graphite monochromator
θ -range (°)	2.94–26.64
<i>hkl</i> range	$-10 \leq h \leq 5$ $-14 \leq k \leq 15$ $-17 \leq l \leq 17$
No. of reflections, R_{int}	5192, 0.0609
No. of unique reflections	1477
Refinement	JANA [13], full matrix least squares on F^2
Number of parameters	75
Goodness of fit	1.03
Final R indices [$I > 3\sigma_I$]	$R = 0.0404$, $wR = 0.0902$
Final R indices [all data]	$R = 0.0873$, $wR = 0.0961$
Largest difference peaks $\Delta\rho_{\text{min}}$ and $\Delta\rho_{\text{max}}$ (e/Å ³)	–2.13, 1.91

Crystallographic data for (CuBr)₂P₈Se₃ have been deposited with the Fachinformationszentrum Karlsruhe, D-76334 Leopoldshafen, Germany, fax: +49-7247-808-666, e-mail: crysdata@fiz-karlsruhe.de. They are available on quoting the depository numbers CSD-413695, the name of the authors and the reference of the publication.

Raman spectra were recorded on a Bruker RFS100/S-Fourier transform spectrometer equipped with a Nd:YAG laser ($\lambda = 1064 \text{ nm}$) and a liquid nitrogen cooled germanium detector. Samples were sealed in Duran glass capillaries of 1 mm outside diameter. The resolution was 2 cm^{-1} . Spectra were processed with the OPUS program package [14].

Table 2

Atomic coordinates and isotropic displacement parameters in Å² for (CuBr)₂P₈Se₃

Atom	Wyckhoff	x	y	z	U_{eq}^a
Br1	4d	0.0837(3)	0.0753(1)	1/4	0.0315(6)
Br2	4d	–0.2701(3)	–0.1250(1)	1/4	0.0324(6)
Se1	4c	–0.0886(2)	–1/4	1/2	0.0265(6)
Se2	8e	0.4204(2)	–0.0767(1)	0.38919(9)	0.0385(5)
Cu1	4d	–0.2061(3)	0.0719(2)	1/4	0.0284(8)
Cu2	4d	0.0078(3)	–0.1250(2)	1/4	0.0258(7)
P1	8e	–0.2549(4)	0.1622(2)	0.3900(2)	0.021(1)
P2	8e	0.0887(4)	–0.1951(2)	0.3924(2)	0.0215(9)
P3	8e	0.4802(4)	–0.2579(2)	0.4188(2)	0.0181(9)
P4	8e	0.2020(4)	–0.0627(2)	0.4777(1)	0.0132(9)

All positions are fully occupied.

^a U_{eq} is defined as one third of the trace of the orthogonalized U_{ij} tensor.

Table 3
Anisotropic displacement parameters in Å² of (CuBr)₂P₈Se₃

Atom	<i>U</i> ₁₁	<i>U</i> ₂₂	<i>U</i> ₃₃	<i>U</i> ₁₂	<i>U</i> ₁₃	<i>U</i> ₂₃
Br1	0.040(1)	0.0194(8)	0.0345(8)	−0.001(1)	0	0
Br2	0.026(1)	0.0211(9)	0.050(1)	−0.0023(9)	0	0
Se1	0.025(1)	0.0288(9)	0.0256(7)	0	0	0.0015(6)
Se2	0.045(1)	0.0344(7)	0.0357(6)	−0.0080(8)	0.0051(7)	0.0039(6)
Cu1	0.047(2)	0.021(1)	0.0170(9)	−0.001(1)	0	0
Cu2	0.031(2)	0.028(1)	0.0178(8)	0.004(1)	0	0
P1	0.030(2)	0.021(1)	0.013(1)	−0.002(1)	−0.000(1)	0.001(1)
P2	0.028(2)	0.022(1)	0.015(1)	0.002(1)	−0.003(1)	0.003(1)
P3	0.019(2)	0.018(1)	0.017(1)	0.001(1)	0.005(1)	0.001(1)
P4	0.026(2)	0.005(1)	0.008(1)	0.000(1)	−0.002(1)	0.0012(9)

3. Results and discussion

3.1. The crystal structure of (CuBr)₂P₈Se₃

(CuBr)₂P₈Se₃ can be regarded as an adduct compound of neutral cage molecules P₈Se₃ and rhombs of Cu₂Br₂. The P₈Se₃ cages are the neutral equivalents of the well known so-called ‘ufosane’ polyphosphide [P₁₁]^{3−}, e.g. [15]. By a formal substitution of the three P[−] atoms of the [P₁₁]^{3−} anion one can easily derive the neutral P₈Se₃ molecule, see Fig. 1. The symmetry of an undistorted P₈Se₃ is *D*₃, namely one *C*₃ axis and three *C*₂ axes perpendicular to the *C*₃ axis. However, to date no crystalline compound is known where the ‘ideal’ *D*₃ symmetry is observed for the [P₁₁]^{3−} anion or the P₈Se₃ cage molecule. This is due to the asymmetrical coordination of the cages in the solid state. A comparison of the structural parameters of the two different cages shows their close relation. Thus, the average distances *d*(P–P) and *d*(P–Se) are almost equivalent, i.e. *d* ≈ 2.23 Å, which is a typical P–P bond length, see Table 4. A ‘height’ of *d*(P1–P1′) = 3.70 Å results for P₈Se₃ and *d* = 3.78 Å for the corresponding P atoms in [P₁₁]^{3−}. The distances for

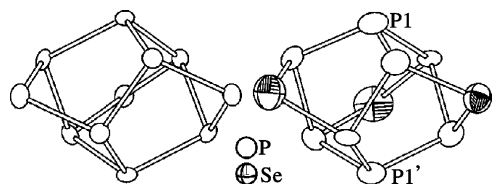


Fig. 1. Molecular structures of [P₁₁]^{3−} and [P₈Se₃]. View parallel to a *C*₂ axis of the *D*₃ symmetrical molecules. The symmetry of the cages is reduced in the crystalline compounds. Data for [P₁₁]^{3−} are taken from Ref. [15].

Table 4
Selected average distances \bar{d} in Å of (CuBr)₂P₈Se₃ and (CuI)₂P₈Se₃

	\bar{d} (P–P)	\bar{d} (P–Se)	\bar{d} (Cu–P)
(CuBr) ₂ P ₈ Se ₃	2.233	2.266	2.259
(CuI) ₂ P ₈ Se ₃	2.230	2.265	2.266

Data taken from Ref. [11].

the atoms defining the ‘tail’ of the molecules, i.e. the Se atoms in P₈Se₃ and the P[−] atoms in [P₁₁]^{3−}, are also within a very narrow range. Thus, *d*(Se–Se) ≈ 5.15 Å and *d*(P[−]–P[−]) ≈ 5.11 Å differ only slightly above the experimental error. These differences become even less meaningful taking into account the different temperatures of 123 K for the structure determination of Cs₃P₁₁·3NH₃ vs. 298 K for (CuBr)₂P₈Se₃. The most prominent difference between the molecular parameters of the two cages is the bond angle of the two-bonded atoms. It varies from 92.9° < ∠(P–Se–P) < 99.5°, and from 95.6° < ∠(P–P[−]–P) < 96.7°.

In (CuBr)₂P₈Se₃ each P₈Se₃ molecule is surrounded by four Cu₂Br₂ rhombs, i.e. four of the eight P atoms are coordinated to one copper atom of each Cu₂Br₂ rhomb. Vice versa each copper atom coordinates to two different P₈Se₃ cages and [Cu₂Br₂P₄] double tetrahedra result. Fig. 2 shows the layered arrangement of P₈Se₃ cages and Cu₂Br₂ rhombs in the crystal structure of (CuBr)₂P₈Se₃.

When the crystal structures of (CuX)₂P₈Se₃ are compared it becomes immediately obvious why only the *a* and *b* lattice parameters differ for X = Br and X = I, respectively. Thus, the different radii of Br[−] and I[−] do not affect the crystal structure along *c* since there are no bonds for the halide ions parallel to this direction. A similar effect

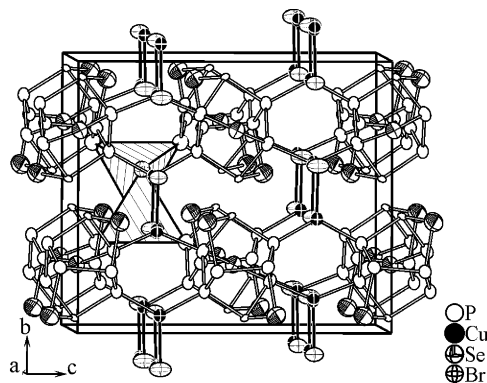


Fig. 2. Section of the crystal structure of (CuBr)₂P₈Se₃. View along layers of P₈Se₃ molecules and Cu₂Br₂ rhombs. Four P₈Se₃ molecules are coordinated by one Cu₂Br₂ rhomb to form edge sharing [Cu₂Br₂P₄] double tetrahedra. Ellipsoids are drawn at an 80% probability level.

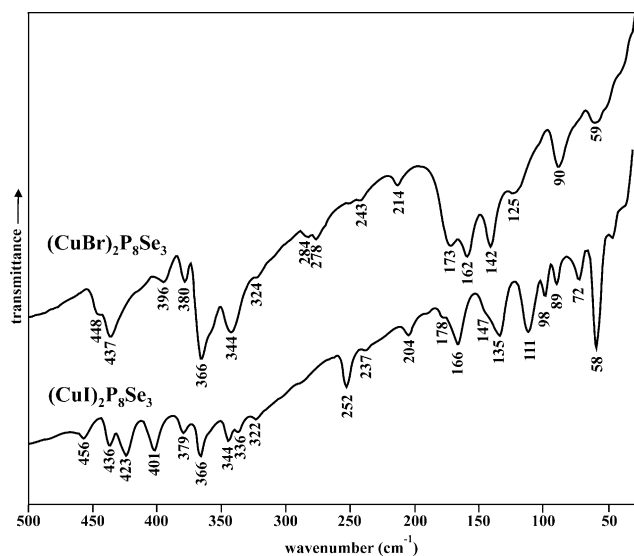


Fig. 3. Far infrared spectra of $(\text{CuBr})_2\text{P}_8\text{Se}_3$ and $(\text{CuI})_2\text{P}_8\text{Se}_3$. Resolution 2 cm^{-1} .

was observed for the homologous pair $(\text{CuI})_3\text{P}_4\text{Se}_4$ and $(\text{CuI})_3\text{P}_4\text{S}_4$ [8,9]. This behavior underlines the adduct character of the compounds under discussion.

3.2. IR and Raman spectroscopic investigations

Due to the isotopic structures of $(\text{CuBr})_2\text{P}_8\text{Se}_3$ and $(\text{CuI})_2\text{P}_8\text{Se}_3$ coming along with almost identical molecular parameters of the P_8Se_3 molecule one can also expect

similar vibrational modes for the molecular parts of the compounds.

From ab initio calculations for numerous phosphorus-selenium molecules [16] and IR and Raman spectroscopic investigations of cage molecules like P_4Q_3 ($\text{Q} = \text{S}, \text{Se}$) [17, 18] the ranges for the wavenumbers of the P–Se and P–P modes have been determined. Vibrational bands can be expected in the range from 530 to 20 cm^{-1} . A gap of about 100 cm^{-1} was observed between the bending modes of P_4Se_3 below 220 cm^{-1} and the stretching modes above 315 cm^{-1} . This gap was also derived from theoretical calculations for phosphorus rich molecules [16]. Transferring these findings to the phosphorus rich P_8Se_3 molecule one should observe a similar separation of bending and stretching modes in $(\text{CuBr})_2\text{P}_8\text{Se}_3$ and $(\text{CuI})_2\text{P}_8\text{Se}_3$.

No bands could be detected above 500 cm^{-1} neither in Raman nor in IR-experiments, see Figs. 3 and 4. The observed frequencies are summarized in Table 5. Focusing on the range between 500 and 300 cm^{-1} the IR spectra of $(\text{CuBr})_2\text{P}_8\text{Se}_3$ and $(\text{CuI})_2\text{P}_8\text{Se}_3$ are almost identical in their relative intensities and positions of

Table 5
Observed Raman and IR modes of $(\text{CuBr})_2\text{P}_8\text{Se}_3$ and $(\text{CuI})_2\text{P}_8\text{Se}_3$

Raman	IR		
$(\text{CuBr})_2\text{P}_8\text{Se}_3$	$(\text{CuI})_2\text{P}_8\text{Se}_3$	$(\text{CuBr})_2\text{P}_8\text{Se}_3$	$(\text{CuI})_2\text{P}_8\text{Se}_3$
		59(w)	58(m)
			72(w)
		90(m)	89(w)
			98(w)
			111(m)
123(vw) ^a	122(w)	125(m) ^a	
	132(m) ^a		135(m) ^a
141(s) ^a	141(w)	142(s) ^a	
158(m) ^a	154(w) ^a		147(w) ^a
	164(m) ^a	162(s) ^a	166(m) ^a
177(m) ^a	176(vs) ^a	173(s) ^a	178(w) ^a
186(m)	186(m)		
216(vs)	206(s,b)	214(w)	204(m)
241(vw)	237(vw)	243(vw)	237(w)
257(w)	253(m)		252(s)
274(m,sh)	265(m)		
278(s)	278(w)	284(w)	
	297(m,b)	287(w)	
328(vw)	322(vw)	324(w)	322(w)
336(vw)	339(s)		336(w)
347(m)	345(m,sh)	344(s)	344(m)
360(w)			
368(w)	368(vs)	366(vs)	366(s)
381(w)		380(m)	379(m)
396(w)	391(w)		
403(w)	405(s)	396(m)	401(s)
418(m)	423(m)		423(s)
430(vw)	436(w)	437(s)	436(m)
441(vw)	451(vw)	448(m)	456(m)
451(w)	461(w)		

P_8Se_3 bending mode region

P_8Se_3 stretching mode region

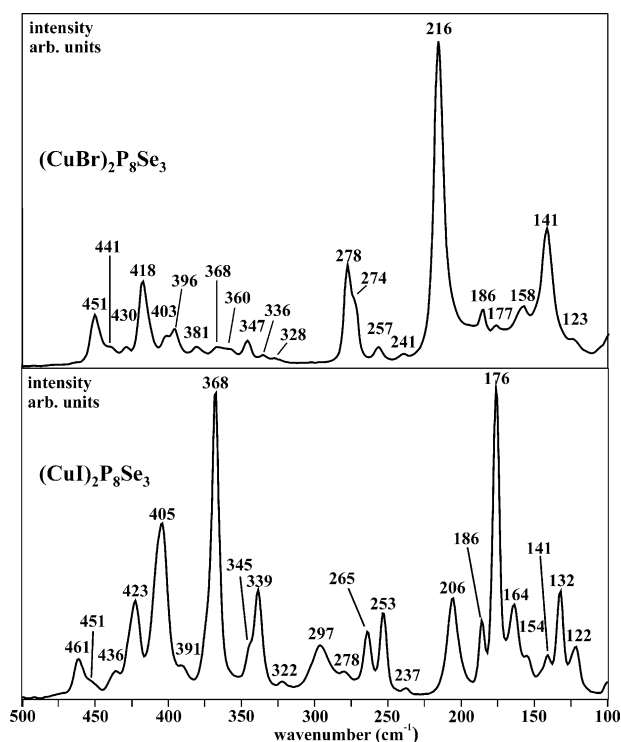


Fig. 4. Raman spectra of $(\text{CuBr})_2\text{P}_8\text{Se}_3$ and $(\text{CuI})_2\text{P}_8\text{Se}_3$. Resolution 2 cm^{-1} .

Intensities: vw, very weak; w, weak; m, middle; s, strong; vs, very strong.

^a Marked frequencies are used for the correlation curve shown in Fig. 5.

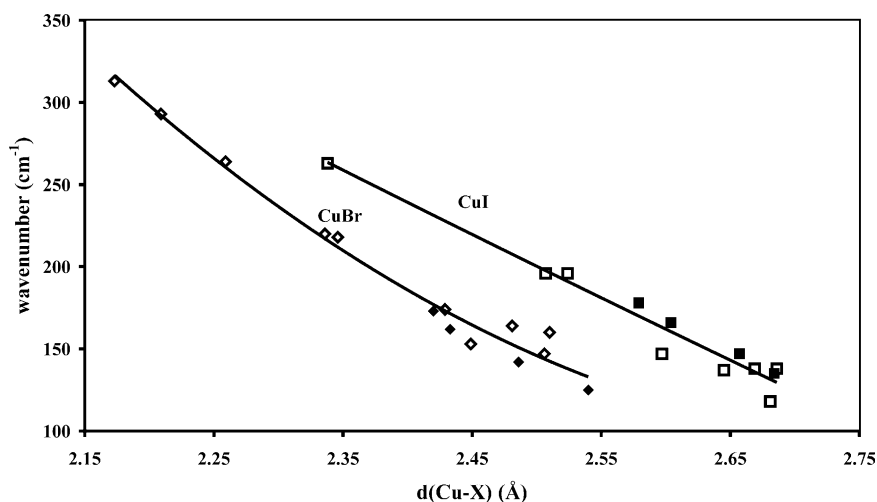


Fig. 5. Plot of the wavenumbers of Cu–X modes vs. Cu–X bond lengths for CuX complexes (data from Ref. [19]) and CuXSe_3 (X = Br, I) [22] (white marks) and $(\text{CuX})_2\text{P}_8\text{Se}_3$ (X = Br, I) (black marks).

the bands, see Fig. 3. This region is supposed to be the stretching mode area of the P_8Se_3 molecule in analogy to the results from other cage molecules like P_4Q_3 (Q = S, Se). Comparing the IR spectra of $(\text{CuBr})_2\text{P}_8\text{Se}_3$ and of $(\text{CuI})_2\text{P}_8\text{Se}_3$ a more pronounced splitting of the bands becomes obvious for $(\text{CuI})_2\text{P}_8\text{Se}_3$. For example, the broad band at 437 cm^{-1} in $(\text{CuBr})_2\text{P}_8\text{Se}_3$ splits into a double band at 436 and 423 cm^{-1} in $(\text{CuI})_2\text{P}_8\text{Se}_3$. The same is found for the bands at 344 and 142 cm^{-1} . However, this effect might be due to a better crystalline sample of $(\text{CuI})_2\text{P}_8\text{Se}_3$ resulting in bands with smaller half-widths since no reduction of symmetry is present.

Contrary to the IR spectra, the relative intensities of the Raman spectra of the two homologous compounds differ quite drastically, see Fig. 4. However, at the present stage we cannot comment on this finding. The pronounced tendency of the splitting of the bands can also be observed in the Raman spectra, e.g. at 418 and 347 cm^{-1} ($(\text{CuBr})_2\text{P}_8\text{Se}_3$).

The bending mode region of the P_8Se_3 molecule as well as the Cu–X stretching mode region can be expected at wavenumbers below 220 cm^{-1} and superimposition cannot be excluded. A separation of bending and stretching mode regions comparable to other phosphorus chalcogenide molecules does not become obvious from the spectra of the compounds under discussion.

A helpful correlation was found to identify the Cu–X modes beside the P_8Se_3 bending modes. The Cu–X stretching modes depend on the bond distances $d(\text{Cu–X})$ in copper(I) halide phosphine complexes [19–21]. The Cu–X stretching modes of 34 complexes containing terminal Cu–X bonds were correlated with the respective Cu–X distances. It was shown that the vibrational frequencies of the Cu–X modes are independent of the nature of the phosphine ligands. Based on this correlation the Cu–X modes of CuBrSe_3 and CuISe_3 reported by Sarfati and Burns [22], i.e. $(\text{CuX})_2\text{Se}_6$ with molecular neutral selenium rings Se_6 , were

clearly identified and the vibrational frequencies were fitted to the distances observed in the crystal structures. These materials show some structural similarities with the compounds under discussion as they also exhibit some kind of copper halide matrix and neutral molecules embedded therein, cf. [1]. Fig. 5 shows the correlation of the data reported in Refs. [19,22] extended by the corresponding data for the compounds under discussion in this work. Due to the excellent fit, the bands at 125 – 173 cm^{-1} are assigned to Cu–Br stretching modes and the bands at 135 – 178 cm^{-1} to Cu–I stretching modes.

Acknowledgements

This work was financially supported by the Deutsche Forschungsgemeinschaft.

References

- [1] A. Pfitzner, Chem. Eur. J. 6 (2000) 1891–1898.
- [2] E. Freudenthaler, A. Pfitzner, Solid State Ionics 101–103 (1997) 1053–1059.
- [3] B. Jayasekera, J.A. Aitken, M.J. Heeg, S.L. Brock, Inorg. Chem. 42 (2003) 658–660.
- [4] G. Brunklaus, J.C.C. Chan, H. Eckert, S. Reiser, T. Nilges, A. Pfitzner, Phys. Chem. Chem. Phys. 5 (2003) 3768–3776.
- [5] A. Pfitzner, E. Freudenthaler, Z. Kristallogr. 210 (1995) 59.
- [6] E. Freudenthaler, A. Pfitzner, Z. Kristallogr. 212 (1997) 103–109.
- [7] T. Nilges, S. Reiser, A. Pfitzner, Z. Anorg. Allg. Chem. 629 (2003) 563–568.
- [8] A. Pfitzner, S. Reiser, Inorg. Chem. 38 (1999) 2451–2454.
- [9] S. Reiser, G. Brunklaus, J.H. Hong, J.C.C. Chan, H. Eckert, A. Pfitzner, Chem. Eur. J. 8 (2002) 4228–4233.
- [10] A. Pfitzner, S. Zimmerer, Z. Kristallogr. 212 (1997) 203–207.
- [11] A. Pfitzner, S. Reiser, T. Nilges, Angew. Chem. 112 (2000) 4328–4330. A. Pfitzner, S. Reiser, T. Nilges, Angew. Chem., Intl. Ed. Engl. 39 (2000) 4160–4162.
- [12] XRed and XShape, Programmes for Numerical Absorption Correction. Stoe and Cie GmbH, Darmstadt, Germany, 1999.

- [13] V. Petricek, M. Dusek, The Crystallographic Computing System JANA2000, Institute of Physics, Praha, Czech Republic, 2000.
- [14] Opus [2.2], Bruker Analytische Messtechnik, Karlsruhe, Germany, 1996.
- [15] D. Knettel, M. Reil, N. Korber, Z. Naturforsch. (B) 56 (2001) 965–969.
- [16] G.M.S. Lister, R. Jones, Phys.: Condens. Matter 1 (1989) 6039–6048.
- [17] M. Somer, W. Bues, W. Brockner, Z. Naturforsch. (B) 35 (1980) 1063–1069.
- [18] J.R. Rollo, G.R. Burns, W.T. Robinson, J.H. Clark, H.M. Dawes, Inorg. Chem. 29 (1990) 2889–2894.
- [19] G. Bowmaker, P.C. Healy, J.D. Kildea, A.H. White, Spectrochim. Acta 44A (1988) 1219–1223.
- [20] G. Bowmaker, R.D. Hart, E.N. de Silva, B.W. Skelton, A.H. White, Aust. J. Chem. 50 (1997) 553–565.
- [21] ($\nu = b(r)^{-m}$ with ν = wavenumber (cm^{-1}), r = bond distance (\AA), $b = 18,000$ (Br) 32,300 (I) and $m = 5.2$ (Br) 5.6 (I)).
- [22] J.D. Sarfati, G.R. Burns, Spectrochim. Acta 50A (1994) 2125–2136.